

# THE MULTIPLE ACCESS INTERFERENCE SIMULATION ON PRN-BASED TWO-WAY SATELLITE TIME TRANSFER

<sup>1</sup>Yi-Jiun Huang, <sup>1,2</sup>Wen-Hung Tseng, <sup>1</sup>Shinn-Yan Lin,  
<sup>1</sup>Huang-Tien Lin, <sup>1</sup>Fang-Dar Chu, and <sup>1</sup>Chia-Shu Liao

<sup>1</sup>Telecommunication Laboratories, Chunghwa Telecom Co., Ltd.  
12, Lane 551, Min-Tsu Rd. Sec. 5, Yang-Mei, Taoyuan, Taiwan 32601  
Tel: +886 3 4244783, Fax: +886 3 4245474, E-mail: *dongua@cht.com.tw*

<sup>2</sup>Institute of Photonics Technologies, National Tsing Hua University, Taiwan

## Abstract

*To perform two-way satellite time transfer (TWSTT), participants use pseudo-random noise (PRN) coded signals to measure the propagation delay from the other site and exchange their measurements. When all participants transmit their PRNs at the same time, multiple access interference (MAI) will exist. The MAI may cause the error in delay measurements, and may even cause the diurnal effect when a geo-stationary satellite is in motion. We conduct numerical simulations to investigate the relation between ground station parameters and the diurnal effect. Our simulation results show that the diurnal effect is related to the PRN carrier frequency offset and chip rate. It is also related to the signal bandwidth and the difference of MAI power. We also find the possibility of diurnal effects is code-dependent and baseline-dependent.*

## INTRODUCTION

Currently, two-way satellite time transfer (TWSTT) provides a precise way to compare the atomic time scales [1]. When performing TWSTT, all participations employ pseudo-random noise (PRN) signals to access the satellite at the same time [2]. Then, participants exchange their time delay measurement data for computing the time-scale differences. A conventional TWSTT with a chip rate of 1 Mcps (chips per second) can provide an accuracy of 1 nanosecond at one day [3].

Based on the orthogonal property of PRN, a superposition of multi-PRN signals can be individually discriminated. However, because PRNs are not absolutely orthogonal, any other superposed PRN may cause errors in propagation delay measurement. The unwanted PRN is called “multiple access interference” (MAI) [4].

Recent research exhibits that the performance of TWSTT is highly limited by the diurnal effect [5,6], which is a time measurement error in diurnal variations. We suppose the MAI would be one of the key factors that result in the diurnal effect when a satellite is in a slight motion. In this paper, we investigate the time measurement error caused by the MAI via the method of numerical simulations. The relation between MAI and the diurnal effect is also discussed.

## ORTHOGONALITY OF PRN

Assuming  $c_1(t)$  and  $c_2(t)$  are two PRN waveforms with the same period  $T$  and the number of linear feedback shift register (LFSR), but generated from different primitive polynomials, they form an orthogonal basis,  $\{c_1(t), c_2(t)\}$  [7]. If their orthogonality is perfect, the cross-correlation of  $c_1(t)$  and  $c_2(t)$  can be expressed as

$$\varepsilon(\tau) = \int_0^T c_1(t)c_2(t-\tau)dt,$$

which must be zero for all  $\tau$ . However,  $\varepsilon(\tau)$  does not always equal to zero, because PRN-formed orthogonal basis is not perfect.

Measurement of propagation delays can be realized by using the PRN signals. In such delay measurements, the method of delay-locked loop (DLL) is widely used in hardware configuration [7,8]. Figure 1 illustrates a delay measurement by using PRN signals. When a PRN travels from a transmitter (TX) to another receiver (RX), an S-curve is generated by the DLL of the receiver. The propagation delay can be measured by finding the zero-crossing of the S-curve. Because PRNs are not absolutely orthogonal [9, 10], any other injected PRN will cause an error in delay measurement, as illustrated in Figure 2.

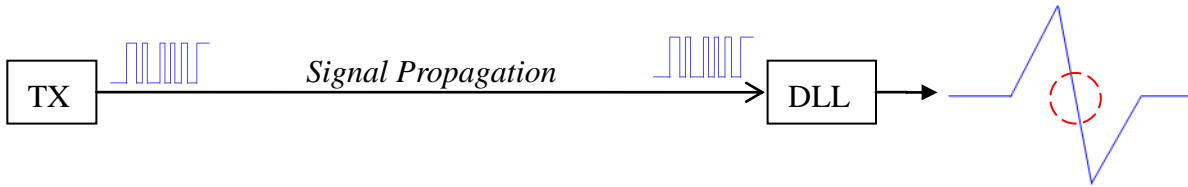


Figure 1. Illustration of delay measurement by using PRN. The DLL is employed to measure the delay by finding the zero-crossing of S-curve within the dashed circle.

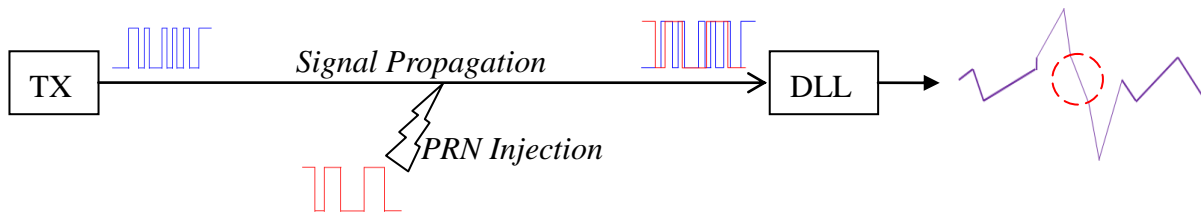


Figure 2. A bias occurred in measured propagation delay when the other PRN is injected.

## MAI ON PRN-BASED TWSTT AND THE DIURNAL EFFECT

The PRN codes are now employed for the operational use of TWSTT [2]. Because PRNs have the orthogonal property, participants with different PRNs can conduct TWSTT using the code-division multiple access (CDMA) configuration. TWSTT participants use a geo-stationary satellite as a communication medium, and measure the time delay of signals from any other sites. By the two-way method, they can get clock difference by exchanging their time delay measurement data.

Figure 3 shows a TWSTT experiment with only one satellite transponder. When conducting TWSTT, participants receive not only desired PRN, but also the unwanted one. A bias in time delay measurement may be caused by unwanted PRNs, called as multiple access interference (MAI). For example, if two participants perform TWSTT, both can get superposition of their PRNs. Their own round-trip PRN becomes the MAI and may lead to a bias in time delay measurement.

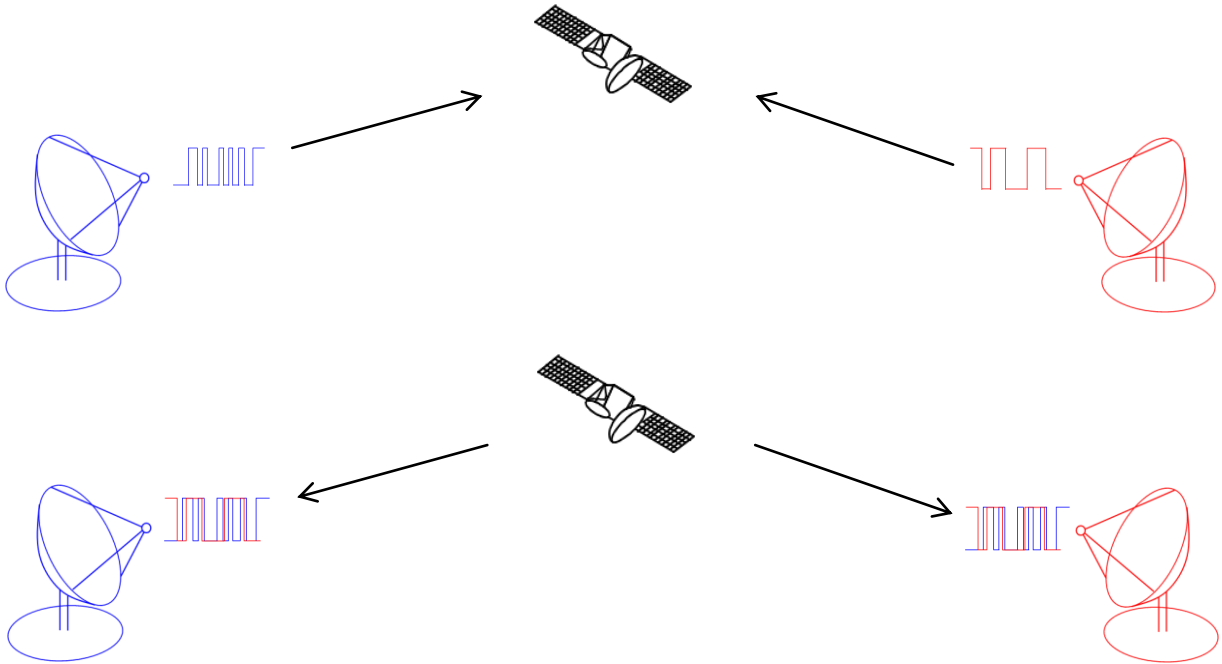


Figure 3. MAI in TWSTT. Participants transmit their PRNs at the same time, and they will also receive MAI (not to scale).

In fact, a geo-stationary satellite is in slight motion to hold itself in a geo-stationary orbit. Therefore, the real orbit and the geo-stationary orbit are slightly different. From the ephemeris data [11], the difference of the real orbit and the geo-stationary orbit displays a daily cycle. MAI may lead to a bias in propagation delay measurement, and the bias may change along with the moving satellite, as shown in Figure 4. Accordingly, we suppose MAI is one of the sources causing the diurnal effect when the geo-stationary satellite is in motion. The following simulations will verify the relationship between the MAI and the diurnal effect.

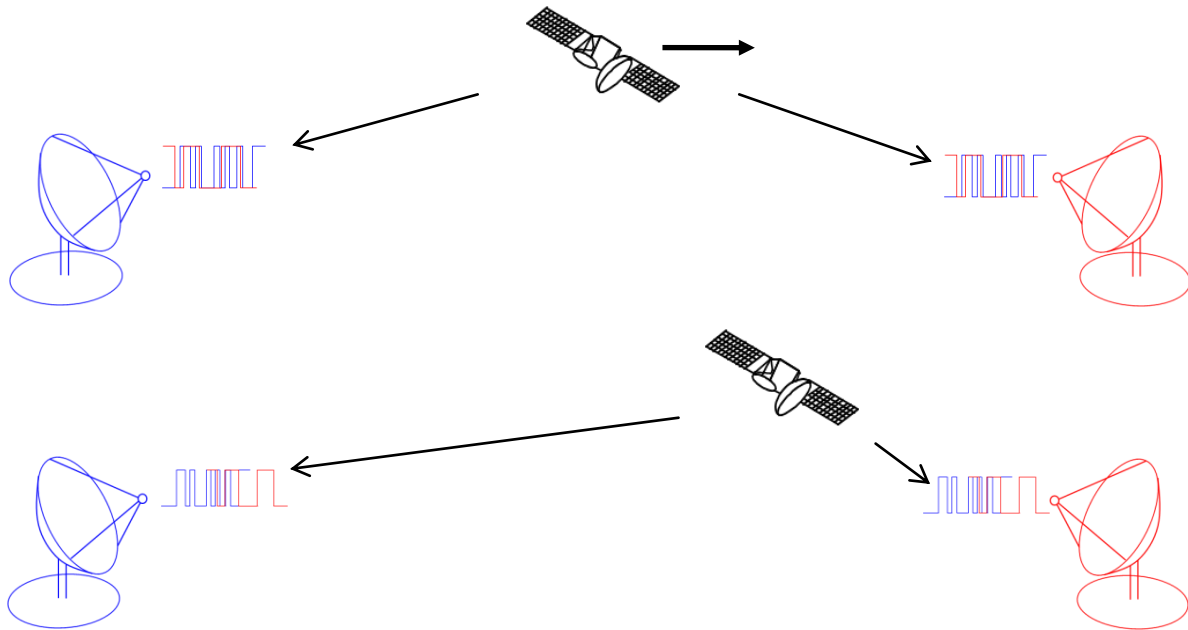


Figure 4. MAI variations along with the moving satellite (not to scale).

## NUMERICAL SIMULATION

To conduct the simulation, we need to set parameters such as propagation delay, PRN number, chip rate, and so on. We refer to the Asia-Pacific TWSTT network and pick two participants, TL and NICT, with their Earth-Centered, Earth-Fixed (ECEF) coordinates. Besides, IS-8 satellite had been treated as the communication medium until Modified Julian Day (MJD) 55651, and the ephemeris is publically available on the Intelsat official website [11]. We use the ephemeris from MJD 55638 to MJD 55646. With those ECEF coordinates, we can get the propagation delay along the TL – IS-8 – NICT path. Other ground station parameters are listed in Table 1.

Table 1. Ground station parameters for numerical simulation.

	Virtual TL* (Site A)	Virtual NICT* (Site B)
PRN number**	PRN #1	PRN #3
Chip Rate	204.6 kcps	204.6 kcps
Carrier Frequency	70 MHz	70 MHz
Signal Bandwidth	409.2 kHz	409.2 kHz

\*ECEF coordinates are available from TWSTT daily reports on the BIPM FTP site [12].

\*\*PRN table is available from [13].

Numerical simulations generate signal waveform with MAI, and measure the propagation delay from site A to site B, and vice versa. The following procedures 1-4 describe how to generate signal waveforms and measure the propagation delay from site B to site A, and the conceptual representation is shown in Figure 5.

1. To obtain the one-way propagation delay from site B to site A, we first get the uplink (U/L) delay calculated by the distance between site B and satellite and divided by the speed of light. In the same way, we calculate the downlink (D/L) delay by the distance between the satellite and site A. Then, the one-way propagation delay from site B to site A is the sum of U/L and D/L delays.
2. To get the round-trip delay at site A, we calculate the ranging delay according to the distance between site A and the satellite. The round-trip delay at site A is double its ranging delay.
3. To generate the received waveform with MAI at site A, we add two signal waveforms from site A and site B. The signal waveform from site A is  $PRN_A$  with the time shift equal to the round-trip delay, modulated by a carrier frequency  $f_A$ . And the signal waveform from site B's TX is  $PRN_B$  with the time shift equal to the one-way propagation delay, modulated by a carrier frequency  $f_B$ .
4. To measure the propagation delay from site B to site A, the received signal waveform is first demodulated by the carrier frequency  $f_B$ , and then correlated with a non-delayed  $PRN_B$  by using a DLL. The propagation delay measurement,  $dt_{B,A}$ , becomes the output from DLL.

By similar procedures, we can also measure the propagation delay,  $dt_{A,B}$ , from site A to B. Therefore, the time-scale difference can be computed by  $(dt_{B,A} - dt_{A,B}) / 2$ .

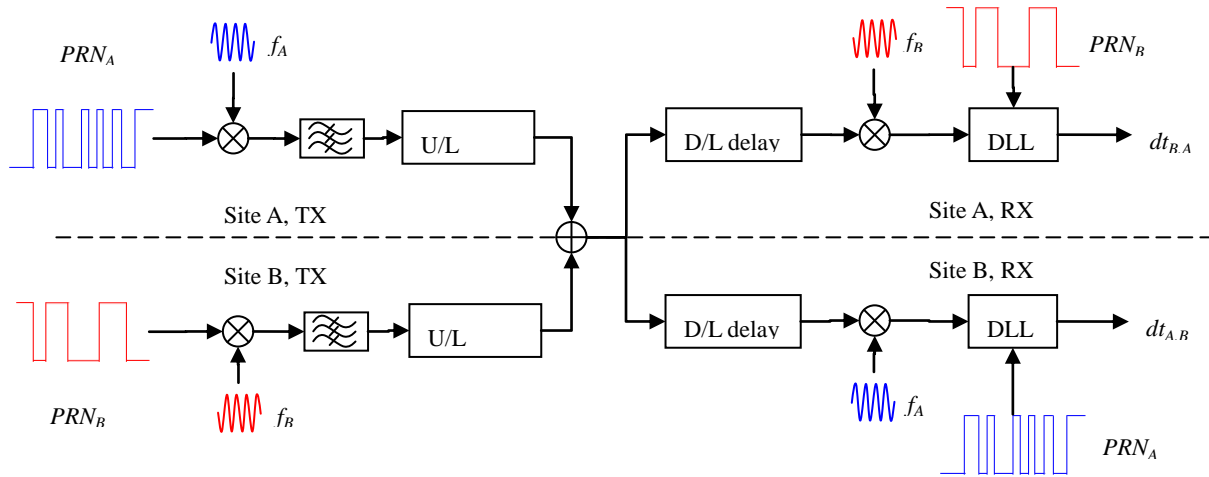


Figure 5. Simulation strategy. Site A measures the propagation delay  $dt_{B,A}$  from site B, while site B measures the propagation delay  $dt_{A,B}$  from site A;  $(dt_{B,A} - dt_{A,B}) / 2$  gives the time-scale difference between site A and site B.

In the following simulation cases, we use different parameter settings for each site. Each case shows time-scale differences changing with date. If the resulting curve is horizontal, then there is no error. Otherwise, there is a measurement error in time-scale differences caused by MAI. We further discuss how much MAI would affect time-scale differences, and focus on the diurnal effect.

### CARRIER FREQUENCY OFFSET

In this case, we set carrier frequency offsets, which are 0 Hz, 1 kHz and 10 kHz, to conduct the TWSTT simulation. The resulting data are drawn in Figure 6. The plot displays that as the offset increases, the diurnal effect will be reduced.

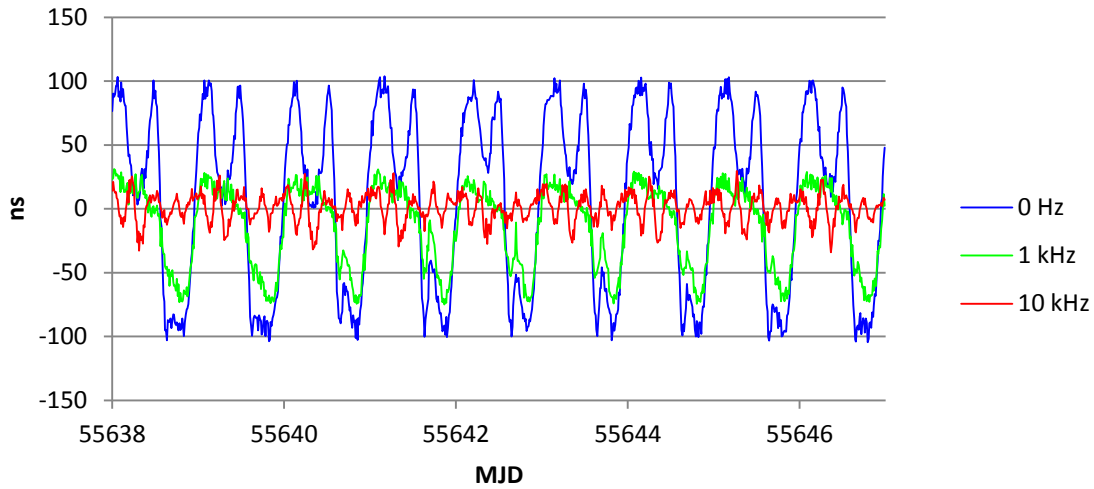


Figure 6. Time-scale difference with different carrier frequency offsets.

### CHIP RATE

In this case, we set chip rates 102.3 kcps, 204.6 kcps and 511.5 kcps, to conduct the TWSTT simulation. The resulting data are drawn in Figure 7. As the chip rate increases, the diurnal effect will be reduced.

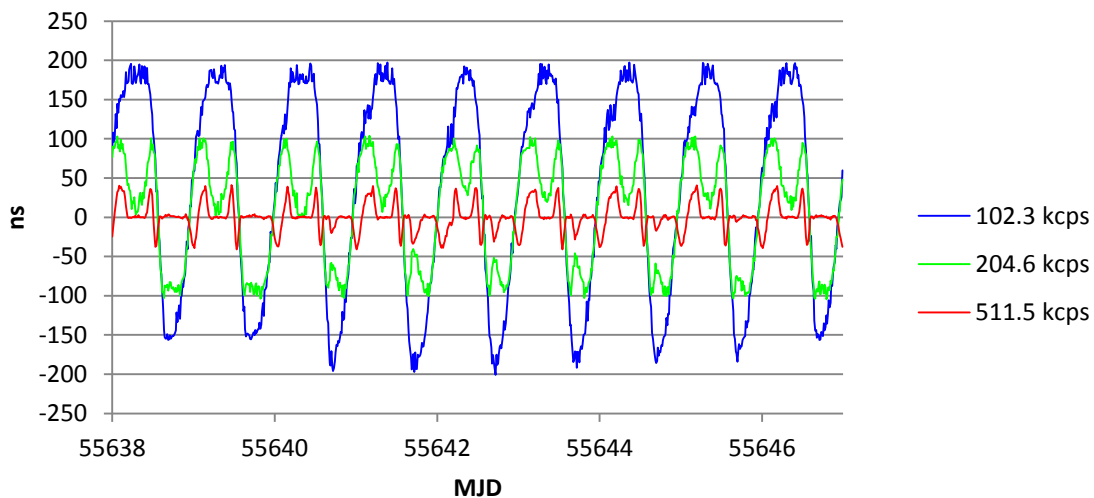


Figure 7. Time-scale difference by using different chip rates.

### SIGNAL BANDWIDTH

In this case, we set signal bandwidths 204.6 kHz, 818.4 kHz and unlimited bandwidth, to conduct the TWSTT simulation. The resulting data are drawn in Figure 8. As the bandwidth increases, the diurnal effect will be reduced.

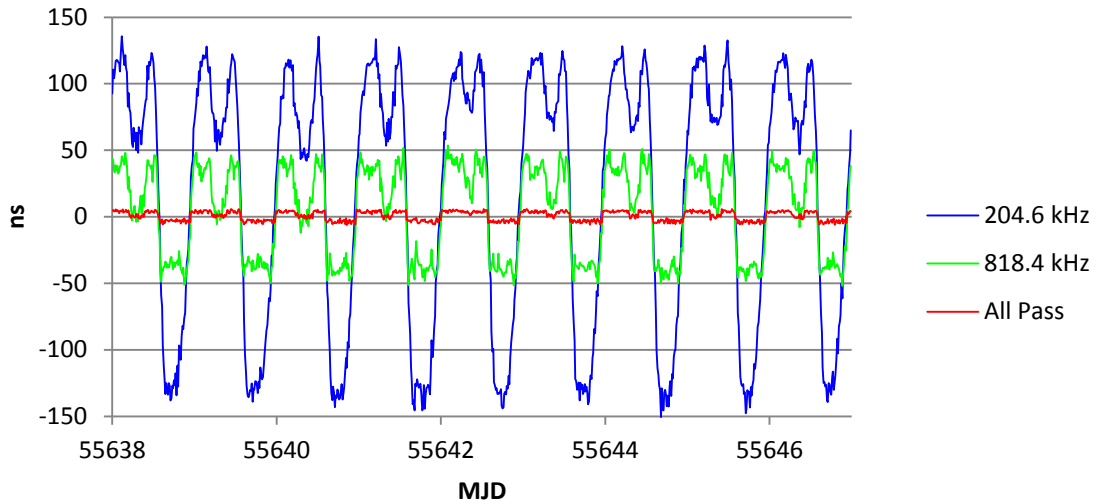


Figure 8. Time-scale difference by using different signal bandwidths.

### MAI POWER DIFFERENCE

In this case, we set transmit power differences 0 dB, 3 dB and 10 dB, to conduct the TWSTT simulation. The resulting data are drawn in Figure 9. As the power levels are balanced, the diurnal effect will be reduced.

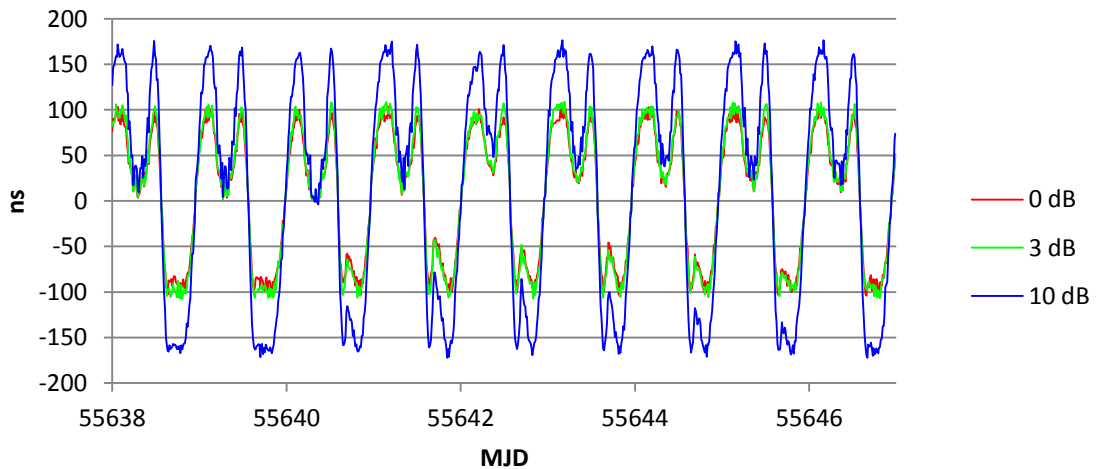


Figure 9. Time-scale difference with different transmit power difference.

## PRN PAIR

In this case, we set PRN pairs (#1, #3), (#1, #4) and (#1, #7), to conduct the TWSTT simulations. The resulting data are drawn in Figure 10. We find that the diurnal effect is significant in the case of (#1, #3) and (#1, #4). Even if we do not change anything except the PRN pair, the diurnal is invisible when using (#1, #7). This simulation indicates the diurnal effect is code-dependent.

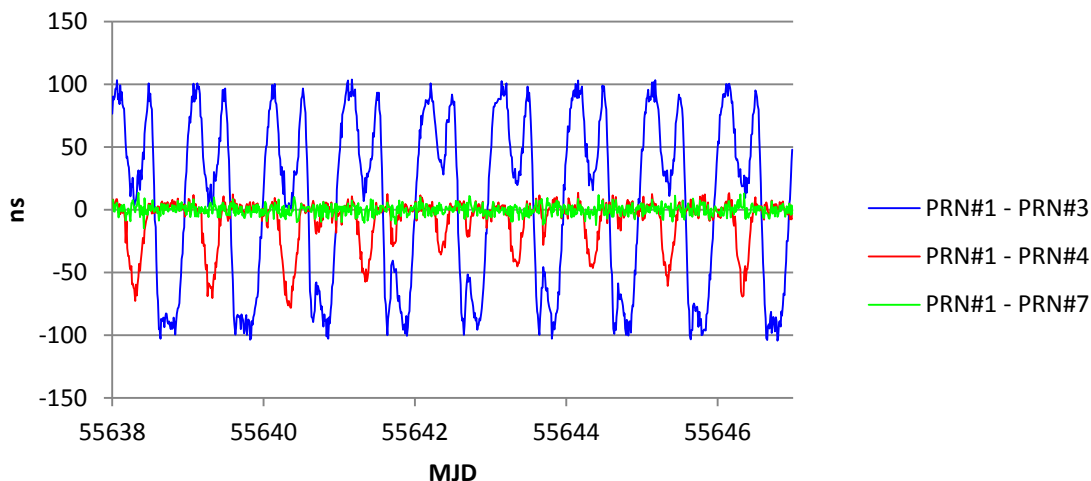


Figure 10. Time-scale difference by using different PRN pairs.

## BASELINE

In this case, we set pairs of participants TL-TL, TL-TL2, TL-NICT and TL-NTSC, to conduct the TWSTT simulations. The related ECEF coordinates can be found TWSTT daily reports on the BIPM FTP site [12]. Each pair of participants uses all of the PRN pairs from PRN#1 to PRN#37, so there are 1332 combinations. Concerning the peak-to-peak time-scale differences within a day, we use the averaged one, listed in Table 2. In Table 2, we find the error in time-scale difference is reduced when the participants get closer. This simulation indicates the diurnal effect is baseline-dependent.

Table 2. Time-scale difference between virtual TL and remote stations.

Remote Station	Baseline (km)	Peak-to-peak time-scale difference (ns)
Virtual TL	0	1.917
Virtual TL2*	276	25.532
Virtual NTSC**	1551	50.693
Virtual NICT	2112	102.072

\*TL2 is a dummy site.

\*\*ECEF coordinates are available from TWSTT daily reports on the BIPM FTP site [12].



## NUMBER OF PARTICIPANTS

In this case, we set numbers of participants to be 2, 3 and 4, to conduct the TWSTT simulations. The resulting data are drawn in Figure 11. This simulation indicates the diurnal effect becomes more pronounced when the number of participants increases.

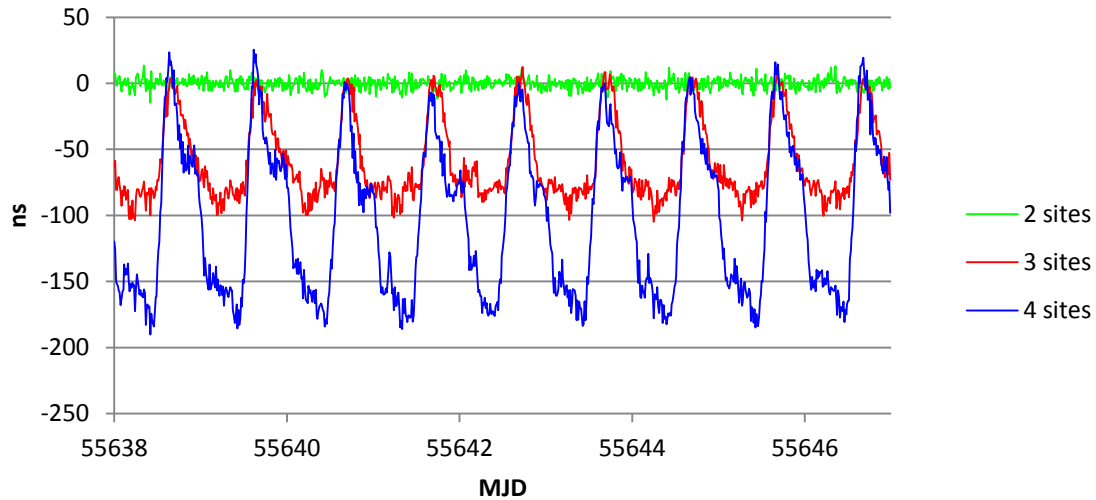


Figure 11. Time-scale difference between virtual TL and NICT, with different numbers of participants.

## CONCLUSION

We have conducted simulations to investigate the relation between MAI and the diurnal effect on PRN-based TWSTT system. Our results demonstrate the amplitude of the diurnal effect strongly depends on different carrier frequency offsets, chip rates, bandwidths and transmit powers. We also found the present of the diurnal effect is probably code-dependent and baseline-dependent. Since the MAI from other participants may lead to the diurnal effect, we should pay attention to reducing its error in the TWSTT system.

## REFERENCES

- [1] D. Kirchner, 1991, "Two-Way Time Transfer via Communication Satellites," **Proceedings of the IEEE**, Vol. 79, No. 7, 983-990.
- [2] ITU Radiocommunication Sector, 2010, "The Operational Use of Two-Way Satellite Time and Frequency Transfer Employing Pseudorandom Noise Codes," ITU-R TF.1153-3.
- [3] V. Zhang, T. E. Parker, J. Achkar, A. Bauch, L. Lorini, D. Matsakis, D. Piester, and D. G. Rovera, 2009, "Two-Way Satellite Time and Frequency Transfer Using 1 MChips/s Codes," in Proceedings of the 41st Annual Precise Time and Time Interval (PTTI) Meeting, 16-19 November 2009, Santa Ana Pueblo, New Mexico, USA, pp. 371-382.

- [4] J. Andrews and T. Meng, 2001, "*Multiple access interference cancellation in fading multipath channels: progress and limitations,*" in Proceedings of the IEEE 53rd Vehicular Technology Conference, Vol. 1, pp. 614-618.
- [5] T. E. Parker and V. Zhang, 2005, "*Sources of Instabilities in Two-Way Satellite Time Transfer,*" in Proceedings of the 2005 Joint IEEE International Frequency Control Symposium (IFCS) and Precise Time and Time Interval (PTTI) Systems and Applications Meeting, 29-31 August 2005, Vancouver, British Columbia, Canada, pp. 745-751.
- [6] D. Piester, A. Bauch, M. Fujieda, T. Gotoh, M. Aida, H. Maeno, M. Hosokawa, and S. H. Yang, 2008, "*Studies on Instabilities in Long-Baseline Two-Way Satellite Time and Frequency Transfer (TWSTFT) Including a Troposphere Delay Model,*" in Proceedings of the 39th Precise Time and Time Interval (PTTI) Systems and Applications Meeting, 27-29 November 2007, Long Beach, California, USA (U.S. Naval Observatory, Washington, D.C.), pp. 211-222.
- [7] R. Peterson, R. Ziemer, and D. Borth, 1995, **Introduction to Spread-Spectrum Communications**, Prentice Hall International, Inc.
- [8] G. Hejc and W. Schaefer, 2009, "*Tracking Biases Caused by Imperfections in DLL Receivers,*" in Proceedings of the 41st Annual Precise Time and Time Interval (PTTI) Meeting, 16-19 November 2009, Santa Ana Pueblo, New Mexico, USA, pp. 551-558.
- [9] D. A. Howe, 1990, "*Time Tracking Error in Direct-Sequence Spread-Spectrum Networks due to Coherence among Signals,*" **IEEE Transactions on Communications**, Vol. 38, No. 12, December 1990, 2103-2105.
- [10] F. G. Ascarrunz, S. R. Jefferts, and T. E. Parker, 1997, "*Earth Station Errors in Two-Way Time and Frequency Transfer,*" **IEEE Transactions on Instrumentation and Measurement**, Vol. 46, No. 2, 205-208.
- [11] Intelsat official website, <http://www.intelsat.com/resources/satellitedata/ephemeris.asp>
- [12] BIPM FTP site, <ftp://tai.bipm.org/>
- [13] PRN table, <http://www.losangeles.af.mil/library/factsheets/factsheet.asp?id=8618>